Supplementary Information (SI) for Analyst.

Supplementary Information

A minimal sampling, in-line spectroscopic calibration method for unstable components during ammoniation of fatty acids

C.M. Raffel, J. Meekes, H.-J. van Manen, A.J.B. ten Kate, A. Chaudhuri,
J. van der Schaaf

August 1, 2024

Contents

S1 Binary mixture of oleic acid and oleic amide **1**

S1.1 Stability of acid and amide mixtures 2

S2 Additional information calibration **2**

S2.1 Composition of calibration samples 2

S2.2 Calibration based on eight samples 2

S3 Ammonia mass flow meter error **4**

S4 Estimation of rate of amide formation **4**

S5 PCA of reaction plateaus **5**

List of Figures

S1 Spectra and compositions of different samples of binary acid-amide mixtures at 120 °C 1

S2 PLS prediction of the calibration and validation experiment based on a PLS calibration of 8 samples 3

S3 Influence of the maximum error by producer of the ammonia mass flow meter on the measured cumulative ammonia content 5

S4 Approximation of amide concentration as a function of time 6

S5 Raw spectra of reaction plateaus 1-6 7

S6 Raw spectra of reaction plateaus 7-9 8

S7 PCA scores and loadings for reaction plateaus 1-3 9

S8 PCA scores and loadings for reaction plateaus 4-6 10

S9 PCA scores and loadings for reaction plateaus 7-9 11

List of Tables

S1 Molar fractions of different binary mixtures of oleic acid and oleic amide at 120 °C . 2

S2 GC-Analysis of a mixture of 1615.15 g oleic acid and 402.38 g oleic amide heated to 120 °C in the reactor, from which samples 1 and 2 were withdrawn and analyzed . . 2

S3 Composition of samples from each dosing step 3

S1 Binary mixture of oleic acid and oleic amide

Experiments with the unreactive binary mixture of oleic acid and oleic amide were performed at 120 °C. 1 kg oleic amide was added to the reactor so that it covered the FT-IR probe and heated while purging with nitrogen to the desired temperature. After stopping the nitrogen purging, oleic acid was added step-wise (steps of ca. 250 g each) to measure the spectra at different compositions. As the mixture was cooled slightly by the addition of oleic acid, it was allowed to heat up until a stable reactor temperature of 120 °C was reached before proceeding to the next oleic acid addition step.

Similar to the ammonia dosing experiments in the previous sections, different compositions of acid and amide were measured. Pure oleic amide was measured in the reactor at 120 °C, to which oleic acid was dosed step-wise, giving in total 12 different mixtures including a pure oleic acid and a pure oleic amide spectrum. Their raw FT-IR spectra in the relevant spectral range from 1820-950 cm^{-1} can be found in Figure S1a and their compositions in Figure S1b as well as Table S1.

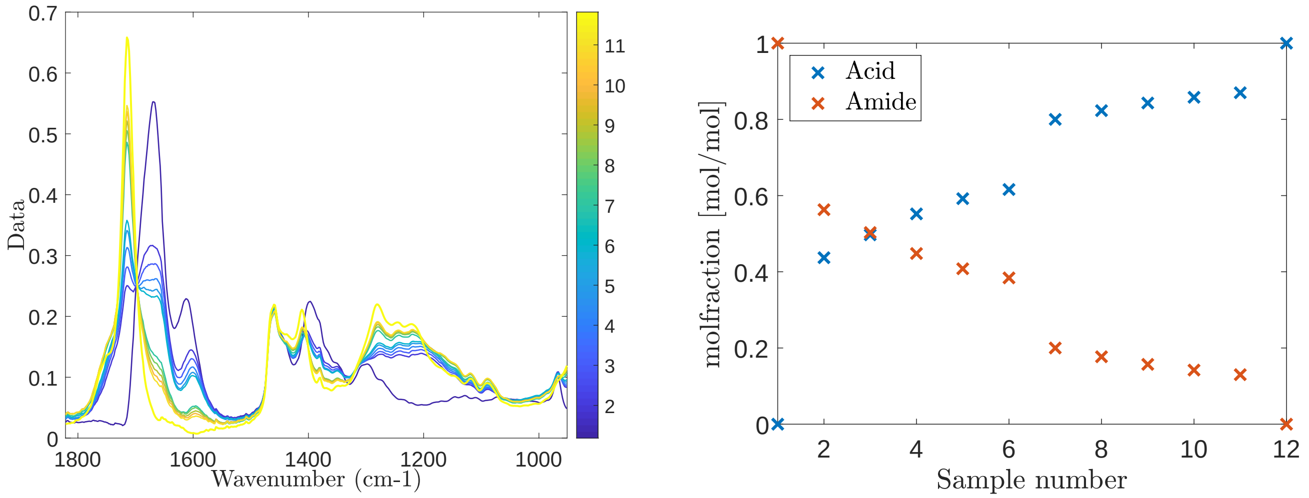

(a) Spectra of 12 binary mixtures of oleic acid and oleic amide at 120 °C

(b) Composition of samples of the binary mixture of acid and amide based on dosing acid to amide

Figure S1: Spectra and compositions of different samples of binary acid-amide mixtures at 120 °C

The composition of acid and amide shown in Figure S1b is given with its exact values in Table S1.

The goal was to use the calibration of the binary mixture of acid and amide in conjunction with the more complicated calibration in the reactive system including ammonia and salt. However, as the addition of ammonia leads to the formation of salt, which is spectrally close to amide, its addition changes the spectral response too fundamentally for this to give satisfactory calibration results.

Table S1: Molar fractions of different binary mixtures of oleic acid and oleic amide at 120 °C

Sample #	x_{acid}	x_{amide}
1	0	1
2	0.437	0.563
3	0.497	0.503
4	0.552	0.448
5	0.592	0.408
6	0.616	0.384
7	0.800	0.200
8	0.823	0.177
9	0.843	0.157
10	0.858	0.142
11	0.870	0.130
12	1	0

S1.1 Stability of acid and amide mixtures

To show that the mixture of oleic acid and oleic amide are indeed nonreactive at 120 °C, a mixture of 80 mol % oleic acid and 20 mol % oleic amide were heated and left to react for more than 2 h. The samples were analyzed with GC, showing in Table S2 that no reaction had taken place and the GC-method works reliably for amide (and acid, as no ammonia was present to form the ammonium salt).

Table S2: GC-Analysis of a mixture of 1615.15 g oleic acid and 402.38 g oleic amide heated to 120 °C in the reactor, from which samples 1 and 2 were withdrawn and analyzed

Sample	t_R [min]	x_{acid}	x_{amide}
0 (weighed)	0	0.8	0.2
1	64	0.8	0.2
2	134	0.8	0.2

S2 Additional information calibration

S2.1 Composition of calibration samples

The exact calculated composition of the eight calibration samples used in Figure 11b is given in Table S3.

S2.2 Calibration based on eight samples

To show the effect that the additional 179 spectra based on the assumptions made in section 3.2 have on the calibration, the calibration was also carried out based only on the eight GC-

Table S3: Composition of samples from each dosing step for calibration

Sample	x_{acid}	x_{amide}	x_{salt}
1	1	0	0
2	0.941	0.006	0.053
3	0.82	0.03	0.15
4	0.752	0.052	0.196
5	0.681	0.075	0.244
6	0.605	0.097	0.298
7	0.457	0.127	0.416
8	0.244	0.162	0.595

samples and their measured and calculated composition. The PLS-model with 4 LVs was applied to the calibration experiment and validation experiment in the same manner as was done for the calibration in Figur 13 and is shown in Figure S2.

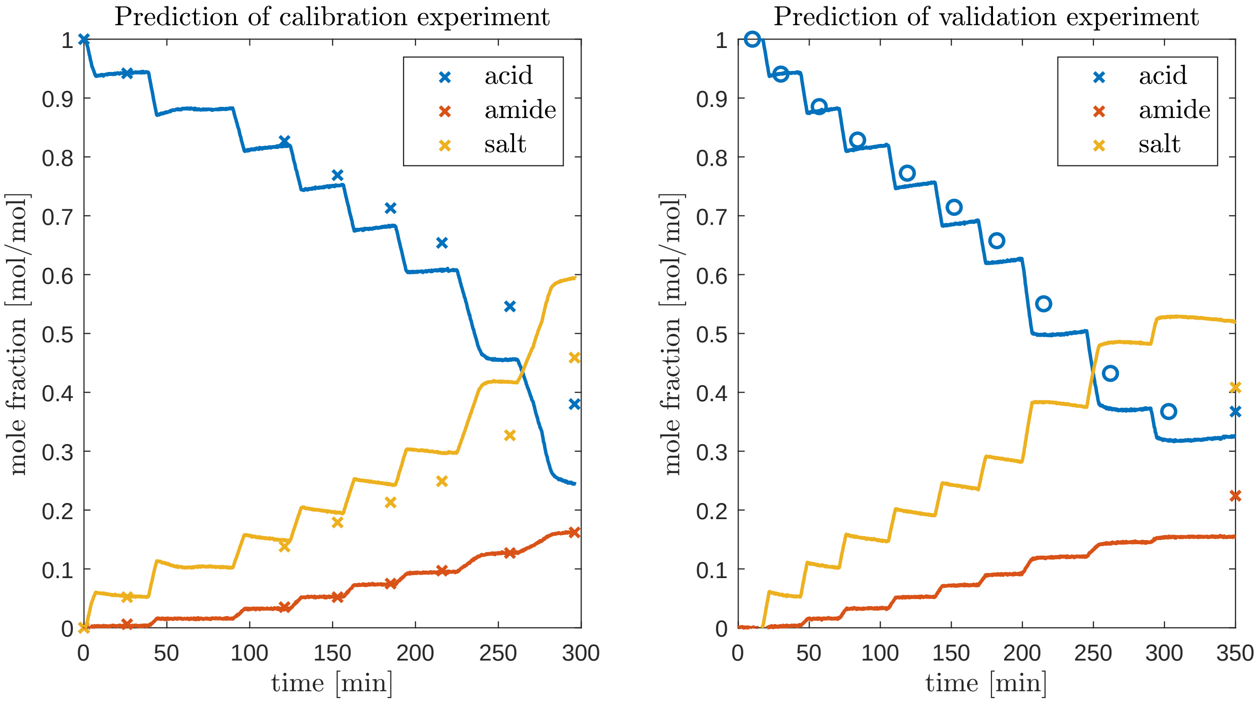

Figure S2: PLS prediction of the calibration and validation experiment based on a PLS calibration of 8 samples. Crosses denote experimental data points, lines the predicted compositions, circles the acid composition from a mass balance with the amount of ammonia dosed.

Figure S2 (left) is able to predict the experimental data points well, as these are the data points used for the calibration itself. The model however struggles predicting a system slightly different from the calibration experiment: the longer the reaction goes on, with each new dosing step, the prediction of the acid content in Figure S2 (right) is worse. The composition in the final sample at 350 min is relatively off, especially for the salt and amide content. Looking at the predicted compositions over time, however, it is evident that the general behavior of the system is captured well. Dosing of ammonia leads to immediate acid consumption and salt formation. At the reaction plateaus, a small amount of salt is consumed, and a small amount of acid is formed again. The predicted composition profile for the amide is less logical. The formation of amide is a slow reaction, as shown in Section 3.2.2. It is therefore unlikely that the amide content increases step-wise during the time of the ammonia dosing, and then stays constant during the reaction plateaus - this is shown in the principal component analysis in Figure 10, where amide formation is observed during the reaction plateaus as the main principal component, as an almost linear function. This is as expected: all ammonia is bound in the form of the salt; whenever a salt reacts back to form acid and molecular ammonia, it can form the amide. This almost linear formation of the amide is not reflected in the prediction from the PLS calibration. It is clear that a higher number of calibration points is necessary to reflect the spectral behavior more accurately with regard to the amide.

S3 Ammonia mass flow meter error

The error of the ammonia mass flow meter can influence the calibration as the amount of ammonia in the system is used in the calibration and is measured via the ammonia mass flow meter. To assess its possible effect, the maximum error by producer is plotted over the course of the reaction in Figure S3. The cumulative ammonia feed is normalized with the initial acid content. The conversion of acid (to either amide or salt) is plotted alongside the cumulative ammonia feed and is based off the calibration in Figure S2. It should correlate with the measured ammonia feed rate. It can be seen that the error of the ammonia MFM is cumulative; the error becomes larger the longer ammonia is dosed. At the beginning of the reaction, the acid conversion and cumulative ammonia fraction are near identical, at later times they diverge slightly more. The difference is much lower than the maximum error by producer would suggest. It is likely that the actual ammonia mass flow controller error is lower, but especially at later reaction times its influence can be visible.

S4 Estimation of rate of amide formation

The slope of the linear function is

$$\frac{dx_{\text{amide}}}{dt} = r_{\text{amide}} = 0.00048254 \tag{1}$$

Integrating with the boundary condition of $x_{\text{amide}}(t = 0) = 0$ leads to

$$x_{\text{amide}} = 0.00048254 \cdot t \tag{2}$$

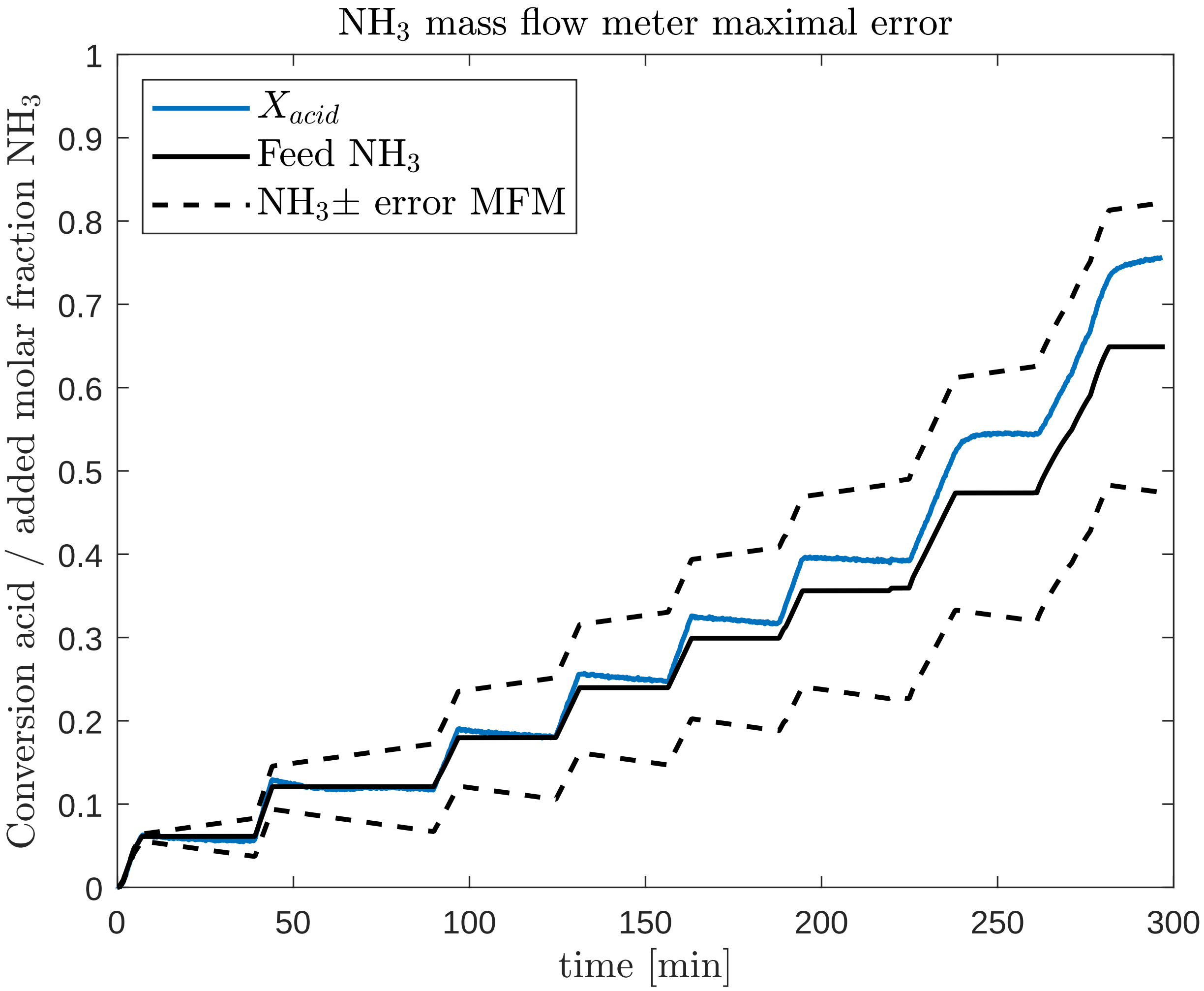

Figure S3: Influence of the maximum error by producer of the ammonia mass flow meter on the measured cumulative ammonia content (normalized to initial amount of acid) and compared to the conversion of acid

sup

S5 PCA of reaction plateaus

The raw spectra of the first and the last reaction plateau are given in Figure 9, they are given here alongside the other spectra plateaus in Figure S5 and S6 (nine in total) in the relevant spectral range.

The results of the PCA analysis performed on these nine reaction plateau spectra is discussed for the first and last plateau in Figure 10, while the PCA results are given as scores and loadings for all plateaus in Figure S7, Figure S8 and Figure S9.

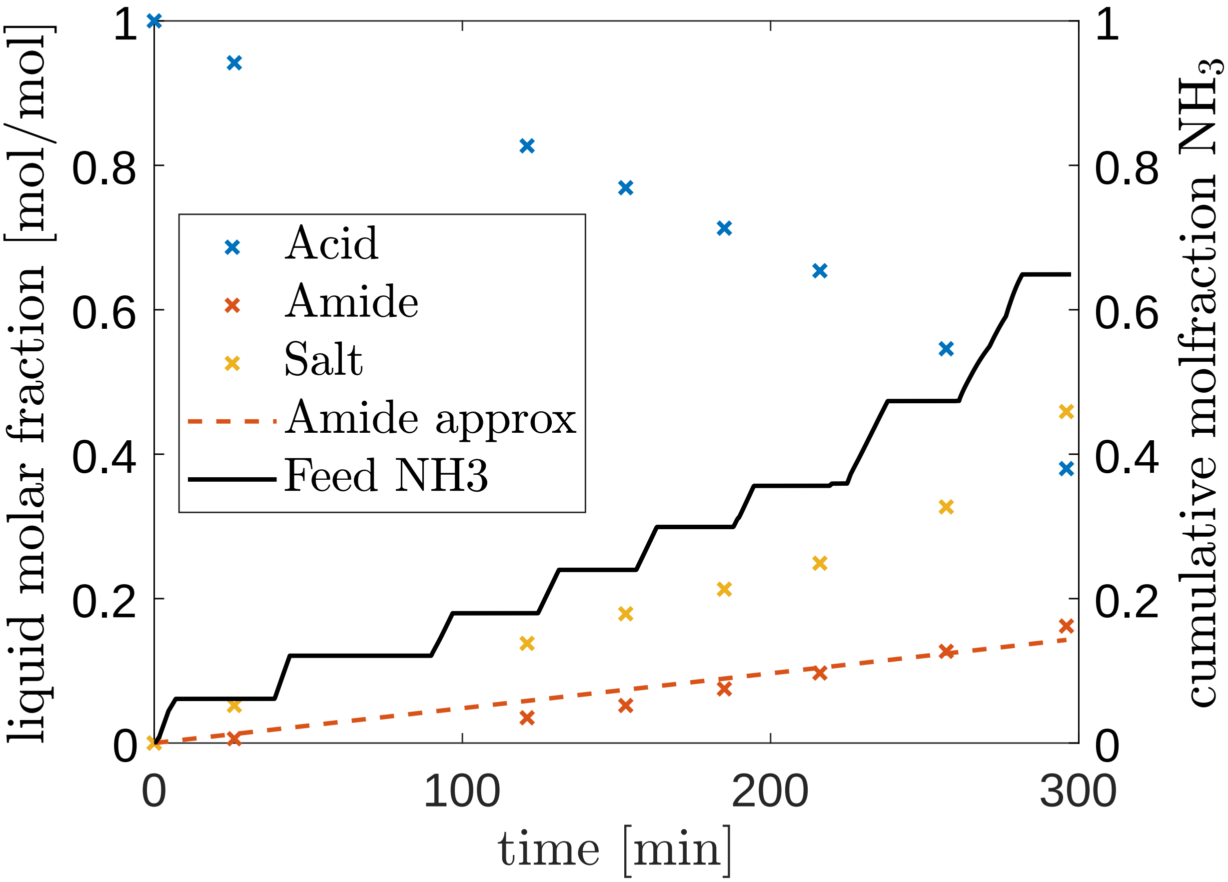

Figure S4: Approximation of amide concentration as a function of time with the slope of the linear function = r_{amide} based solely on amide content from GC-analysis

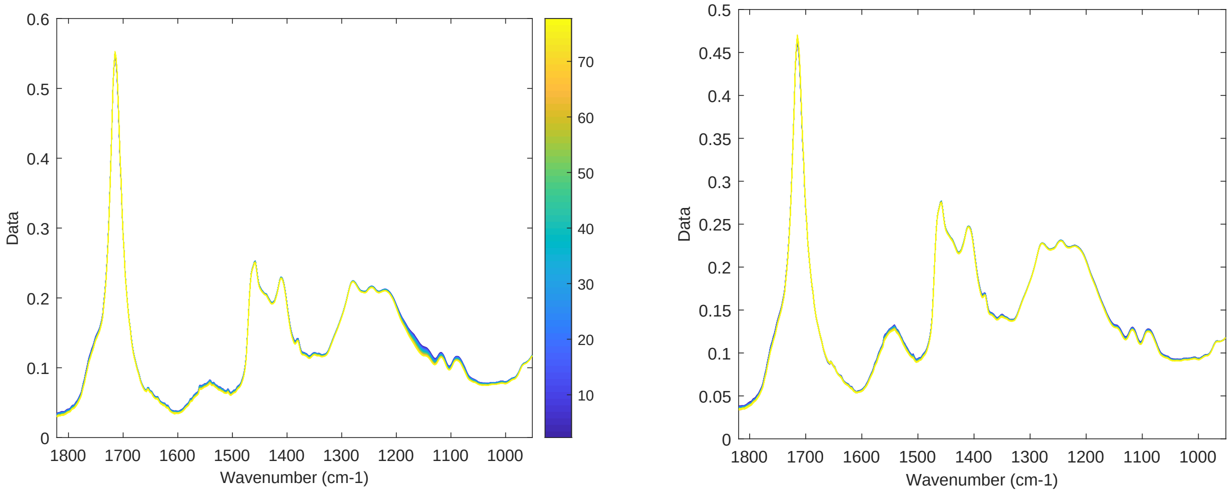

(a) Plateau 1

(b) Plateau 2

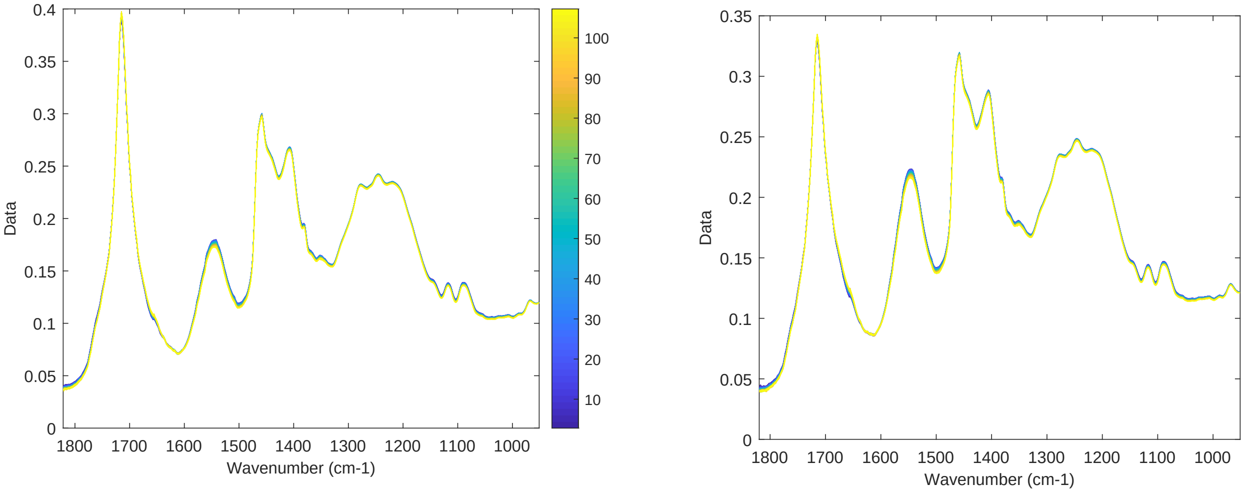

(c) Plateau 3

(d) Plateau 4

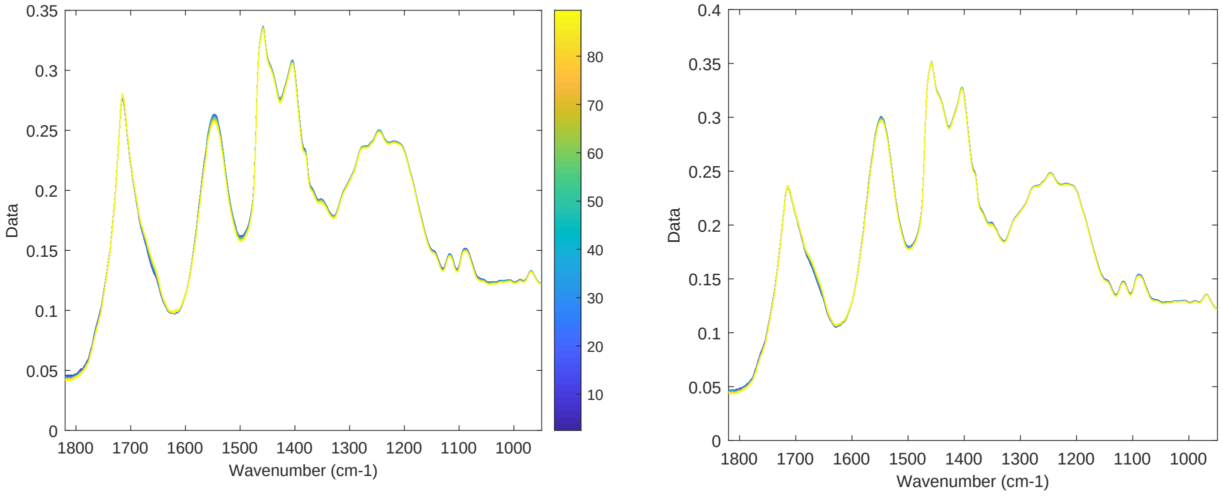

(e) Plateau 5

(f) Plateau 6

Figure S5: Raw spectra of reaction plateaus 1-6

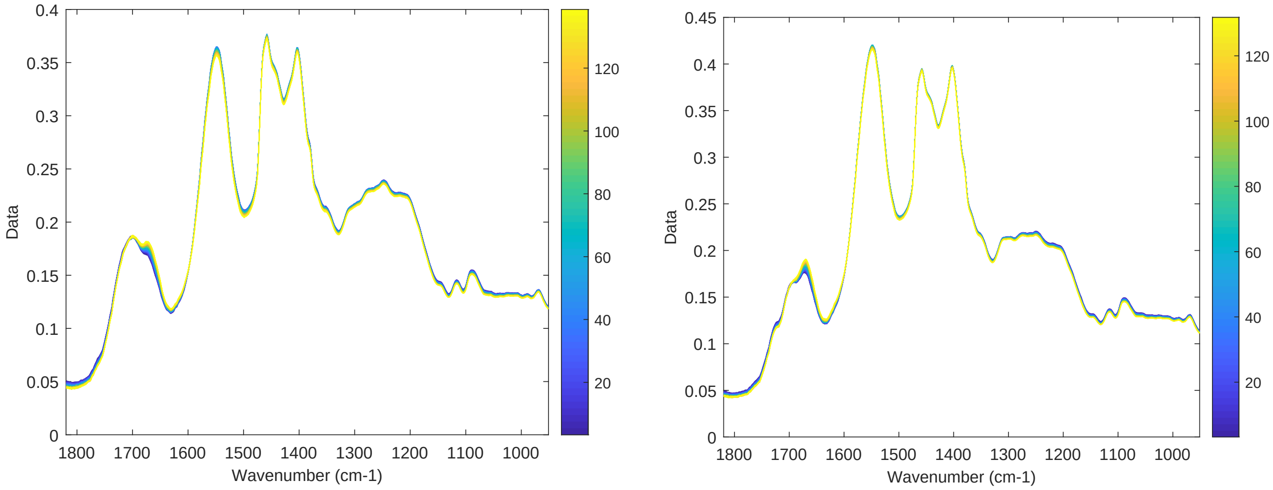

(a) Plateau 7 (b) Plateau 8

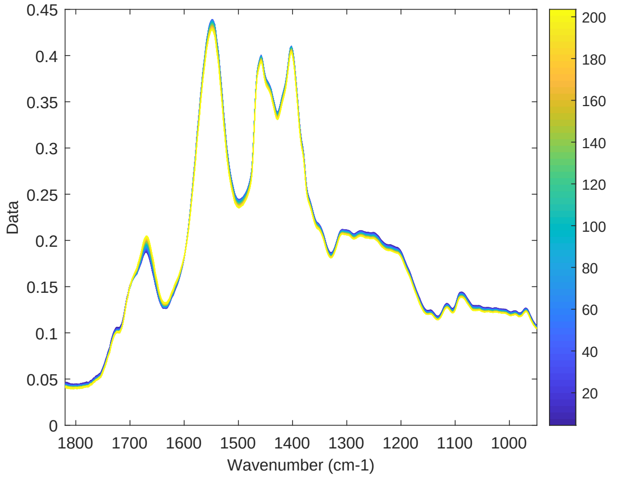

(c) Plateau 9

Figure S6: Raw spectra of reaction plateaus 7-9

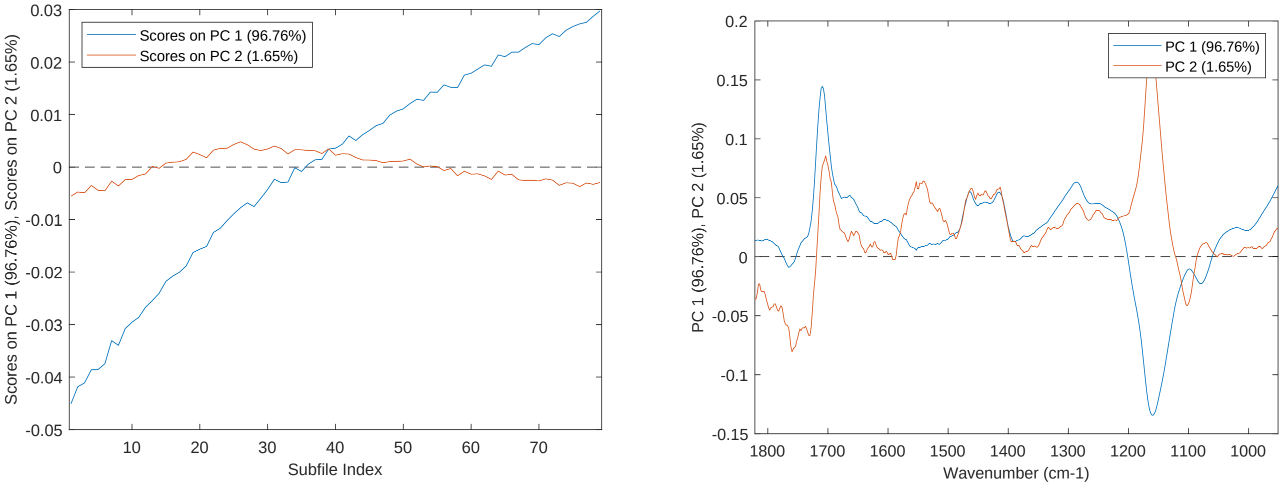

(a) Scores plateau 1 (b) Loadings plateau 1

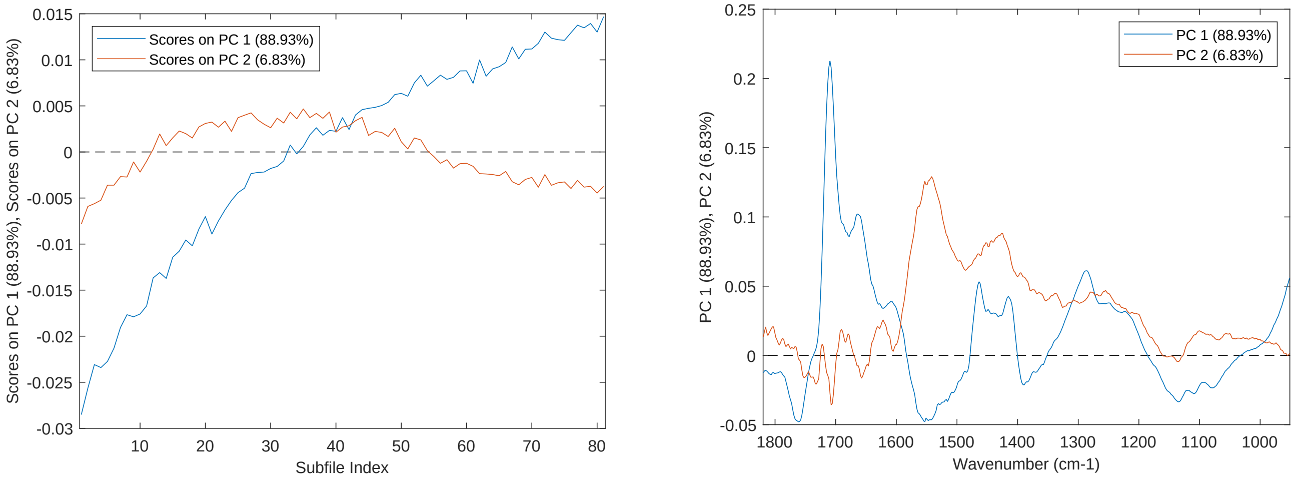

(c) Scores plateau 2 (d) Loadings plateau 2

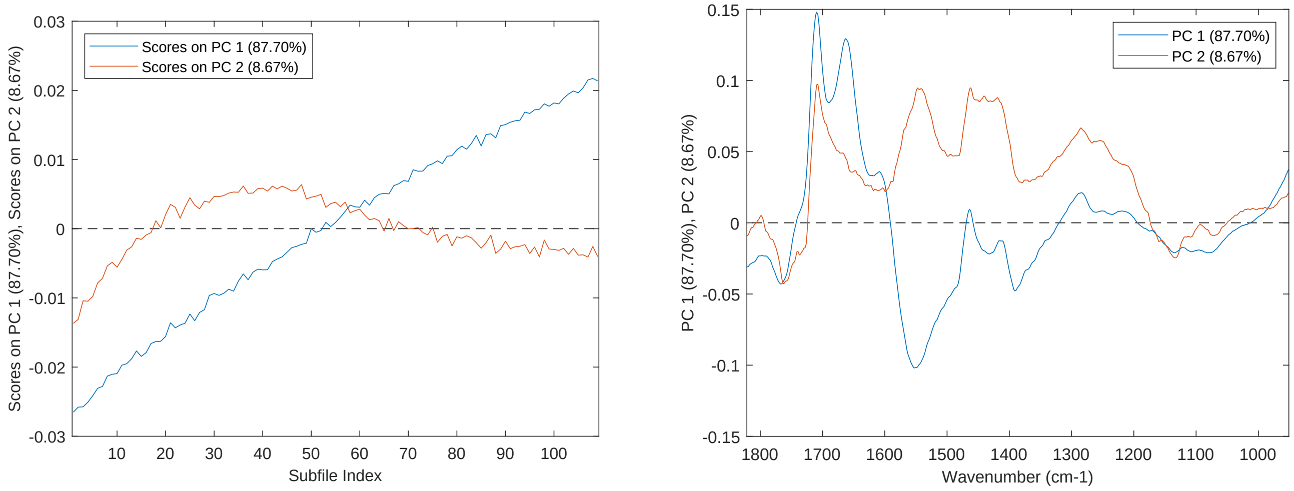

(e) Scores plateau 3 (f) Loadings plateau 3

Figure S7: PCA scores and loadings for reaction plateaus 1-3

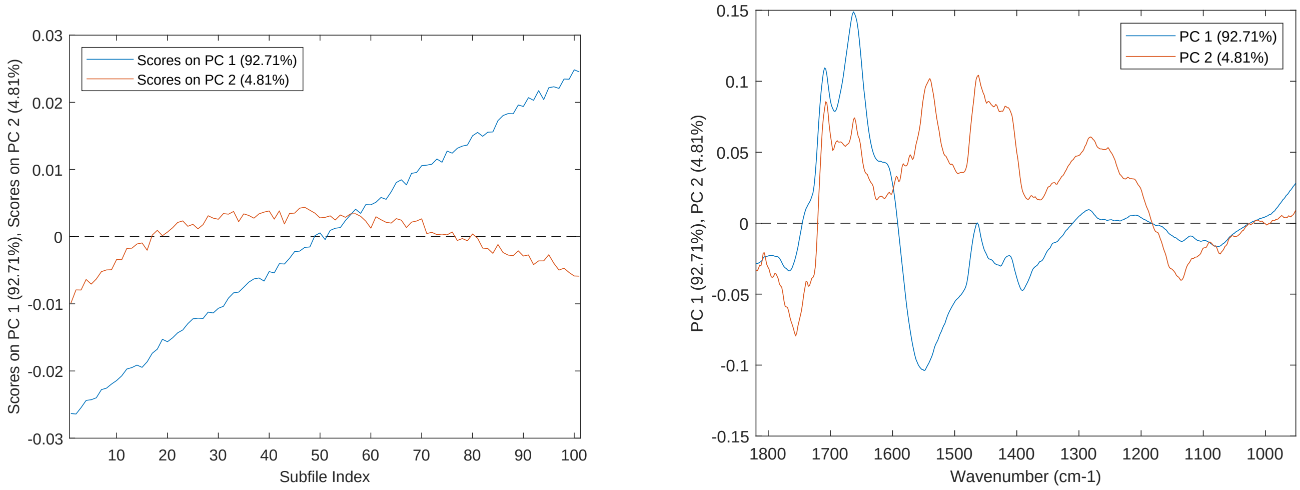

(a) Scores plateau 4

(b) Loadings plateau 4

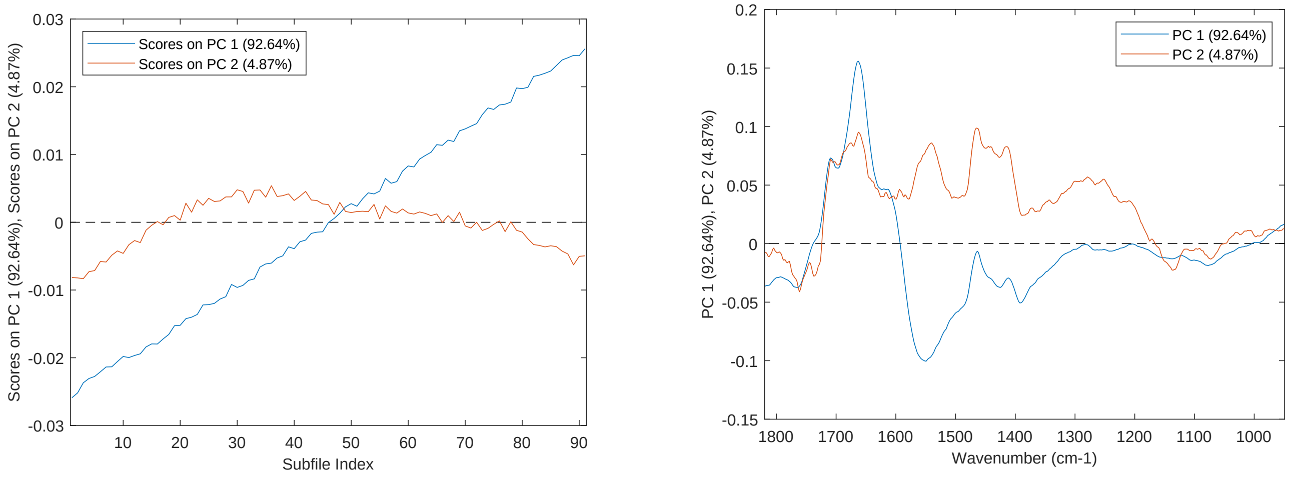

(c) Scores plateau 5

(d) Loadings plateau 5

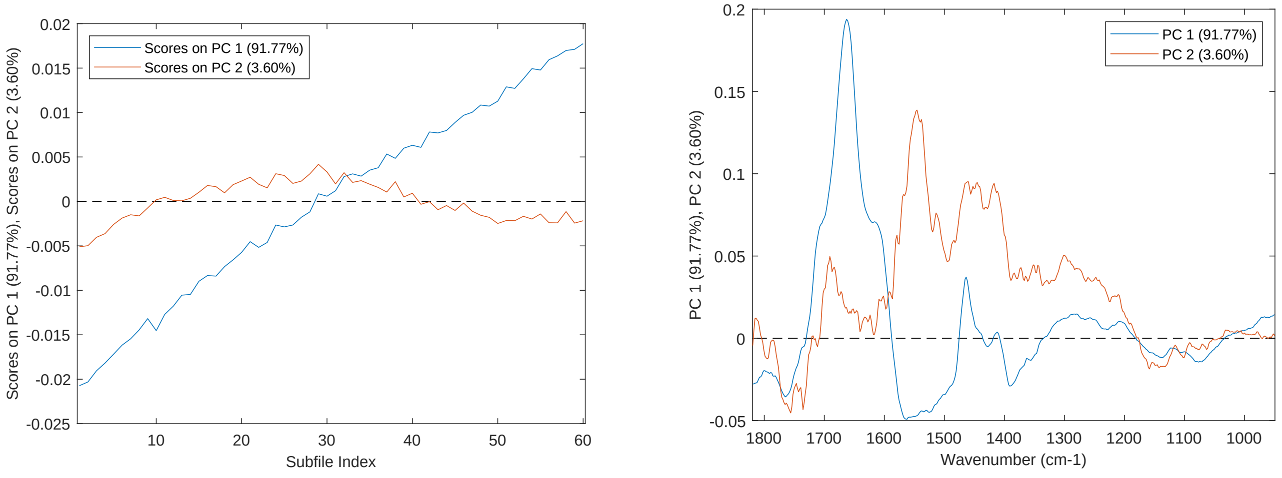

(e) Scores plateau 6

(f) Loadings plateau 6

Figure S8: PCA scores and loadings for reaction plateaus 4-6

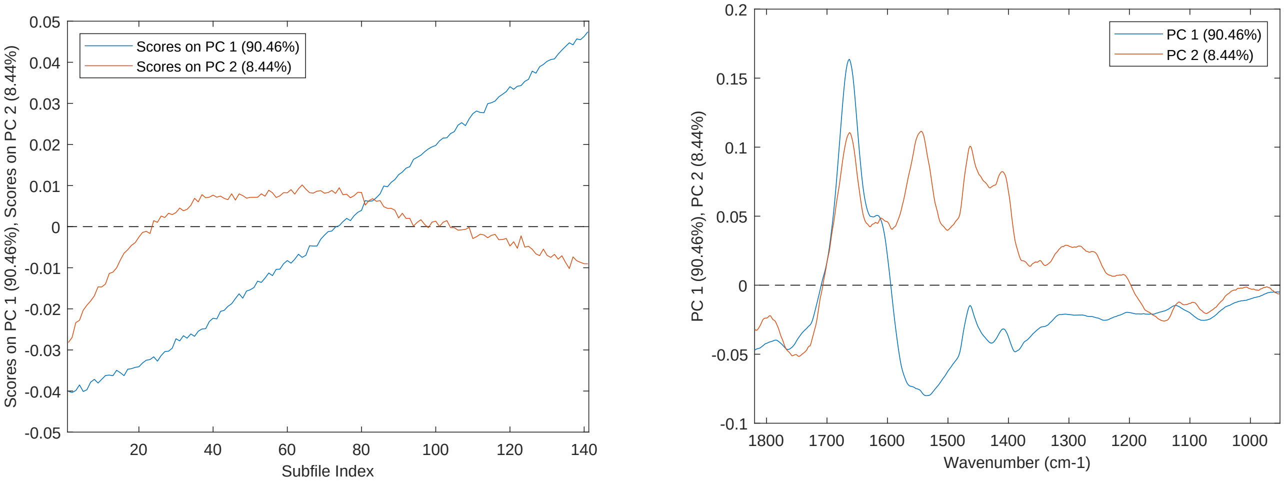

(a) Scores plateau 7

(b) Loadings plateau 7

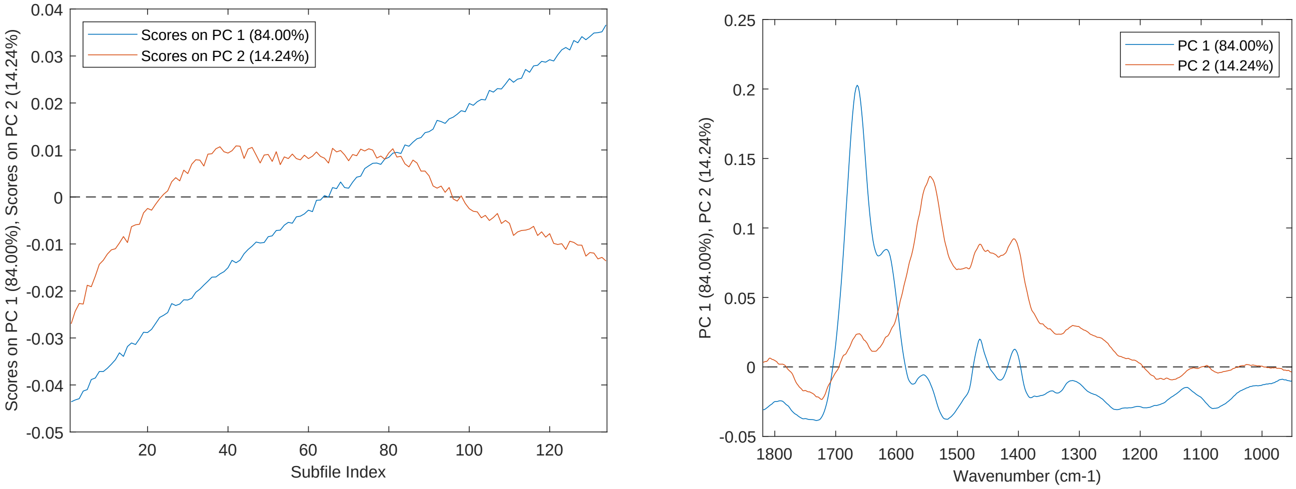

(c) Scores plateau 8

(d) Loadings plateau 8

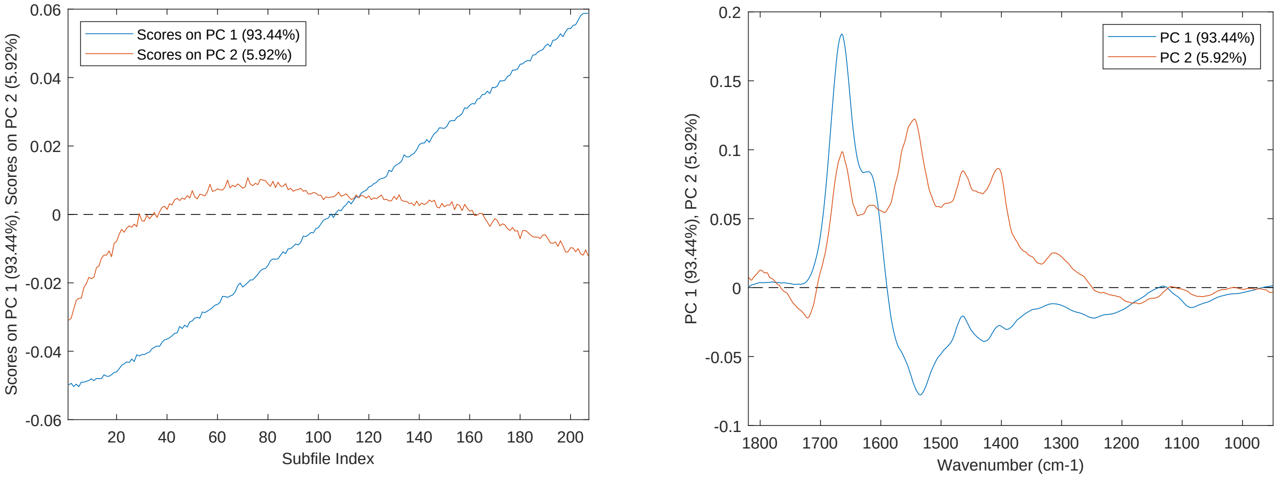

(e) Scores plateau 9

(f) Loadings plateau 9

Figure S9: PCA scores and loadings for reaction plateaus 7-9